© 2014. Published by The Company of Biologists Ltd | Development (2014) 141, 3772-3781 doi:10.1242/dev.108274

RESEARCH ARTICLE

A regulatory network controls nephrocan expression and midgut patterning

Juan Hou[1,*,‡], Wei Wei[1,‡], Ranajeet S. Saund[2], Ping Xiang[1], Thomas J. Cunningham[3], Yuyin Yi[1,4], Olivia Alder[1], Daphne Y. D. Lu[1], Joanne G. A. Savory[5], Nicole A. J. Krentz[1], Rachel Montpetit[1], Rebecca Cullum[1], Nicole Hofs[1], David Lohnes[5], R. Keith Humphries[1,6], Yojiro Yamanaka[7], Gregg Duester[3], Yukio Saijoh[2] and Pamela A. Hoodless[1,4,8,§]

ABSTRACT

Although many regulatory networks involved in defining definitive endoderm have been identified, the mechanisms through which these networks interact to pattern the endoderm are less well understood. To explore the mechanisms involved in midgut patterning, we dissected the transcriptional regulatory elements of nephrocan (*Nepn*), the earliest known midgut specific gene in mice. We observed that *Nepn* expression is dramatically reduced in *Sox17*$^{-/-}$ and *Raldh2*$^{-/-}$ embryos compared with wild-type embryos. We further show that *Nepn* is directly regulated by Sox17 and the retinoic acid (RA) receptor via two enhancer elements located upstream of the gene. Moreover, *Nepn* expression is modulated by Activin signaling, with high levels inhibiting and low levels enhancing RA-dependent expression. In *Foxh1*$^{-/-}$ embryos in which Nodal signaling is reduced, the *Nepn* expression domain is expanded into the anterior gut region, confirming that Nodal signaling can modulate its expression *in vivo*. Together, Sox17 is required for *Nepn* expression in the definitive endoderm, while RA signaling restricts expression to the midgut region. A balance of Nodal/Activin signaling regulates the anterior boundary of the midgut expression domain.

KEY WORDS: Midgut definitive endoderm, Nephrocan (Nepn), Retinoic acid, Sox17, Nodal/Activin A, Mouse

INTRODUCTION

The definitive endoderm (DE), one of the three primary germ layers formed during gastrulation, gives rise to a vast array of highly specialized epithelial cell types that line the respiratory and digestive systems, and which contribute to associated organs, such as thyroid, thymus, lungs, liver, pancreas, stomach and intestines. Before the onset of gastrulation, the mouse embryo is a cup-shaped bilayer, composed of an inner epiblast layer of columnar epithelial cells and an outer visceral endoderm (VE) layer of epithelial cells. Gastrulation is initiated at approximately embryonic day (E) 6.5, when epiblast cells undergo an epithelial-to-mesenchymal transition (EMT) and migrate through the primitive streak to form either mesoderm or DE (reviewed by Nowotschin and Hadjantonakis, 2010). Cells that will contribute to the pluripotent endodermal layer of the embryo undergo a rapid mesenchymal-to-epithelial transition (MET) and intercalate with the VE. Following gastrulation, morphogenetic movements transform the naïve DE, with the integrated VE, into a primitive gut tube. Morphogenesis involves invagination of the foregut and hindgut pockets, expansion of the pockets towards the posterior and anterior, respectively, and closure of the intervening midgut region upon embryonic turning at E9.0 (Lewis and Tam, 2006).

Nodal, a member of the TGFβ family of ligands that includes TGFβs, Activins and BMPs, is essential for gastrulation and formation of mesoderm and DE, with higher levels of Nodal promoting DE formation rather than mesoderm (Vincent et al., 2003). Anterior-to-posterior patterning of the DE is initiated by both the time and position of cell ingression along the primitive streak (Lawson, 1999), with the earliest cells to emerge being directed to the foregut. Gradients of Nodal signaling can also regulate patterning within the DE, with high levels specifying foregut endoderm (Norris et al., 2002). Embryos deficient in *Foxh1*, a transcription factor that mediates a Nodal auto-regulatory circuit resulting in high levels of Nodal, cannot form foregut endoderm, although midgut and hindgut endoderm are present (McKnight et al., 2010). However, the fate of the endoderm is not fully determined at this stage, as transplantation of posterior endoderm to anterior regions can acquire anterior characteristics and vice versa (Wells and Melton, 2000; Kimura et al., 2007). Further endoderm patterning is controlled by a series of reciprocal interactions with nearby mesoderm tissues and the various regions becoming determined at different times around somitogenesis. The broad gene expression patterns within the foregut, midgut and hindgut become progressively refined into precise domains in which specific organs will form (Zorn and Wells, 2009; Kraus and Grapin-Botton, 2012).

In addition to Nodal, DE formation is controlled by a core group of transcription factors, including Eomesodermin [Eomes, eomesodermin homolog (*Xenopus laevis*) – Mouse Genome Informatics], Foxa2 and Sox17. Eomesodermin is required for specification of DE and limits the expression of mesoderm genes (Arnold et al., 2008; Teo et al., 2011). Embryos deficient in *Foxa2*, a forkhead transcription factor, fail to form foregut endoderm, although midgut and hindgut endoderm are present (Dufort et al., 1998; McKnight et al., 2010), a phenotype similar to *Foxh1*$^{-/-}$ embryos (Hoodless et al., 2001; Yamamoto et al., 2001). By contrast, embryos lacking *Sox17*, an HMG-box transcription factor, exhibit deficiencies in gut endoderm in which mid- and hindgut tissues fail to expand (Kanai-Azuma et al., 2002). Endoderm patterning is further refined with several transcription factors

[1]Terry Fox Laboratory, BC Cancer Agency, Vancouver, British Columbia, V5Z 1L3, Canada. [2]Department of Neurobiology and Anatomy, University of Utah, Salt Lake City, UT 84132-3401, USA. [3]Development, Aging and Regeneration Program, Sanford-Burnham Medical Research Institute, La Jolla, CA 92037, USA. [4]Cell and Developmental Biology Program, University of British Columbia, Vancouver, British Columbia V6T 1Z4, Canada. [5]Cellular and Molecular Medicine, University of Ottawa, Ottawa K1H 8M5, Canada. [6]Experimental Medicine, University of British Columbia, Vancouver, British Columbia V6T 1Z4, Canada. [7]Goodman Cancer Research Centre, Department of Human Genetics, McGill University, Montreal, Quebec H2W 1S6, Canada. [8]Department of Medical Genetics, University of British Columbia, Vancouver, British Columbia V6T 1Z4, Canada.
*Present address: STEMCELL Technologies, Inc., Vancouver, British Columbia, V5Z 1B3, Canada.
‡These authors contributed equally to this work

§Author for correspondence (hoodless@bccrc.ca)

Received 23 January 2014; Accepted 8 August 2014

Development (2014) 141, 3772-3781 doi:10.1242/dev.108274

defining specific domains for organogenesis, such as Cdx2 for intestine and colon, Hex1 (Hhex – Mouse Genome Informatics) for liver and thyroid, Pdx1 for pancreas and duodenum and Nkx2-1 for lung (reviewed by Grapin-Botton, 2008). However, the patterning mechanisms after endoderm formation but before organ-specific development are poorly understood.

Endoderm and mesoderm exchange instructive signals that induce specific anteroposterior identities as well as permissive signals required for organogenesis from previously patterned fields. Many growth factor pathways, including FGF, BMP, Wnt and retinoic acid (RA), play multiple stage-specific roles (reviewed by Duester, 2008; Zorn and Wells, 2009; Kraus and Grapin-Botton, 2012). In mouse and chick embryos, FGF4 promotes *Cdx* expression in the hindgut and represses expression of *Hex* and *Foxa2* in the foregut (Wells and Melton, 2000; Dessimoz et al., 2006). Wnt initiates posteriorization, acting directly on endoderm to induce *Cdx2* (Gregorieff et al., 2004; McLin et al., 2007; Goessling et al., 2008; Li et al., 2008; Sherwood et al., 2011). Recently, Engert et al. reported that Wnt/β-catenin signaling also regulates endoderm formation through Sox17 (Engert et al., 2013). In zebrafish, *Xenopus* and chick, BMP posteriorizes the endoderm (Tiso et al., 2002; Wills et al., 2008). In zebrafish and *Xenopus*, RA is important to establish the foregut-midgut boundary (Stafford and Prince, 2002; Chen et al., 2004), and in mouse RA generated in the mesoderm is required for dorsal pancreas formation (Molotkov et al., 2005). RA is also required for posterior endoderm fate establishment (Bayha et al., 2009). Despite studies implicating many signaling pathways in DE patterning, less is known about the mechanisms that link these pathways and how the effects of the different signaling pathways are integrated during endoderm patterning.

We previously identified a novel domain-specific marker, nephrocan (*Nepn*) (Hou et al., 2007), which is first expressed at E7.25 in a limited population of posterior endodermal cells. At E8.0-8.5, expression becomes restricted to the definitive endoderm in the open region of the gut tube between the anterior and posterior intestinal portals. Here, we refer to this region as midgut, and *Nepn* is the earliest known marker specific to this region. By E9.5, *Nepn* is expressed in the dorsal pancreas and duodenum. In adult mice, *Nepn* is expressed in the kidney. Nepn is a member of the small leucine-rich repeat protein (SLRP) family, which includes Biglycan and Decorin. Nepn can act as a secreted inhibitor of TGFβ signaling (Mochida et al., 2006), suggesting a potential functional importance in endoderm development in mice.

Nepn provides a unique opportunity to explore the mechanisms guiding formation and patterning of the midgut DE. We previously showed that two crucial endoderm regulators, *Foxa2* and *Foxh1*, are not required for *Nepn* expression and midgut DE formation in the mouse embryo (McKnight et al., 2010). Here, we describe *in vivo* and *in vitro* experiments examining the mechanisms regulating *Nepn* expression. Our results demonstrate that *Nepn* expression is directly upregulated by RA and Sox17 in a cooperative fashion. Moreover, *Nepn* expression exhibits a concentration-dependent response to Activin signaling, with low levels inducing expression and high levels inhibiting expression. Together, regulation of the midgut-specific gene *Nepn* demonstrates that a network composed of TGFβ family ligands, RA and Sox17, cooperatively patterns the midgut DE.

RESULTS

Sox17 directly induces *Nepn* expression in midgut definitive endoderm

To explore the molecular mechanisms that pattern the midgut endoderm, we analyzed the regulation of *Nepn* gene expression. As

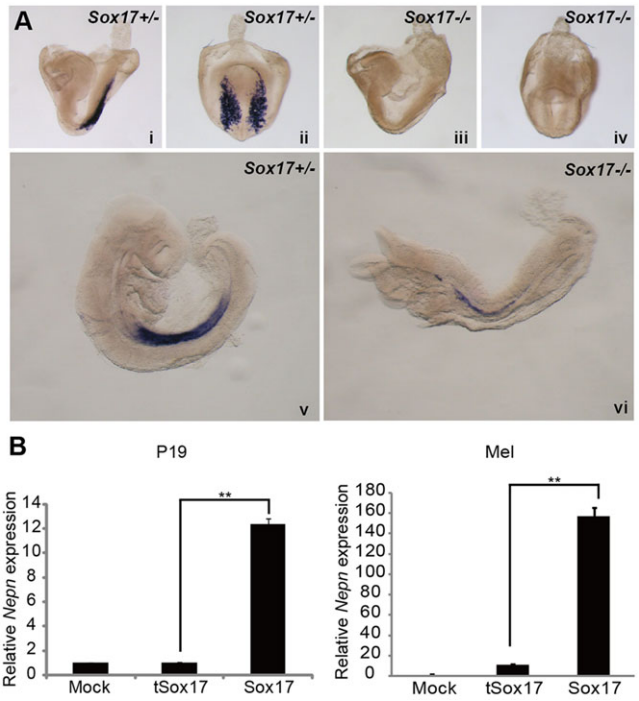

Fig. 1. Sox17 regulates *Nepn* expression. (A) WISH showing *Nepn* expression in $Sox17^{-/-}$ and $Sox17^{+/-}$ embryos at E8.25 (side views i and iii, posterior views ii and iv) and E9.25 (side views v and vi). *Nepn* is substantially downregulated in $Sox17^{-/-}$ embryos. (B) Quantitative RT-PCR of *Nepn* mRNA in P19 and MEL cells transfected with vectors ectopically expressing Sox17, a truncated isoform of Sox17 (tSox17) or mock transfected. Samples were normalized to *β-actin* expression. *Nepn* expression is upregulated in the presence of Sox17.

the transcription factor Sox17 is essential for mid- and hindgut expansion, we first examined *Nepn* expression in $Sox17^{-/-}$ mice. At E8.25, *Nepn* expression was completely lost in $Sox17^{-/-}$ embryos, demonstrating that *Sox17* is necessary for induction of *Nepn* expression, thus supporting previous data showing that Sox17 is required in midgut formation (Fig. 1Ai-iv). Of interest, expression of *Nepn* was observed at E9.25 in $Sox17^{-/-}$ embryos, but was dramatically reduced compared with a heterozygous control (Fig. 1Av,vi), suggesting that factors other than Sox17 can induce *Nepn* expression at later stages.

As *Nepn* expression is downstream of Sox17 during endoderm development, we next explored the mechanisms through which Sox17 regulates *Nepn*. First, we screened several cell lines for endogenous *Nepn* expression (supplementary material Fig. S1A) and selected the murine erythroleukemia cell line (MEL), in which *Nepn* is expressed, and the embryonic carcinoma cell line (P19), with undetectable *Nepn* expression, for further study. To determine whether Sox17 can regulate *Nepn* expression *in vitro*, we ectopically expressed *Sox17* in the cell lines. Supporting the above *in vivo* data, enforced expression of *Sox17* was able to upregulate endogenous *Nepn* expression both in MEL and P19 cells (Fig. 1B). A truncated isoform of Sox17 (tSox17), that lacks part of the HMG domain and thus lacks DNA-binding ability (Kanai et al., 1996), did not induce *Nepn* expression, demonstrating that induction of *Nepn* is dependent on Sox17 transcriptional activity.

To determine if *Nepn* can directly respond to *Sox17* expression, we generated a series of luciferase reporter constructs containing the *Nepn* promoter, including the transcriptional start site (TSS) and various sizes of upstream genomic regions up to −4.7 kb. The

Development (2014) 141, 3772-3781 doi:10.1242/dev.108274

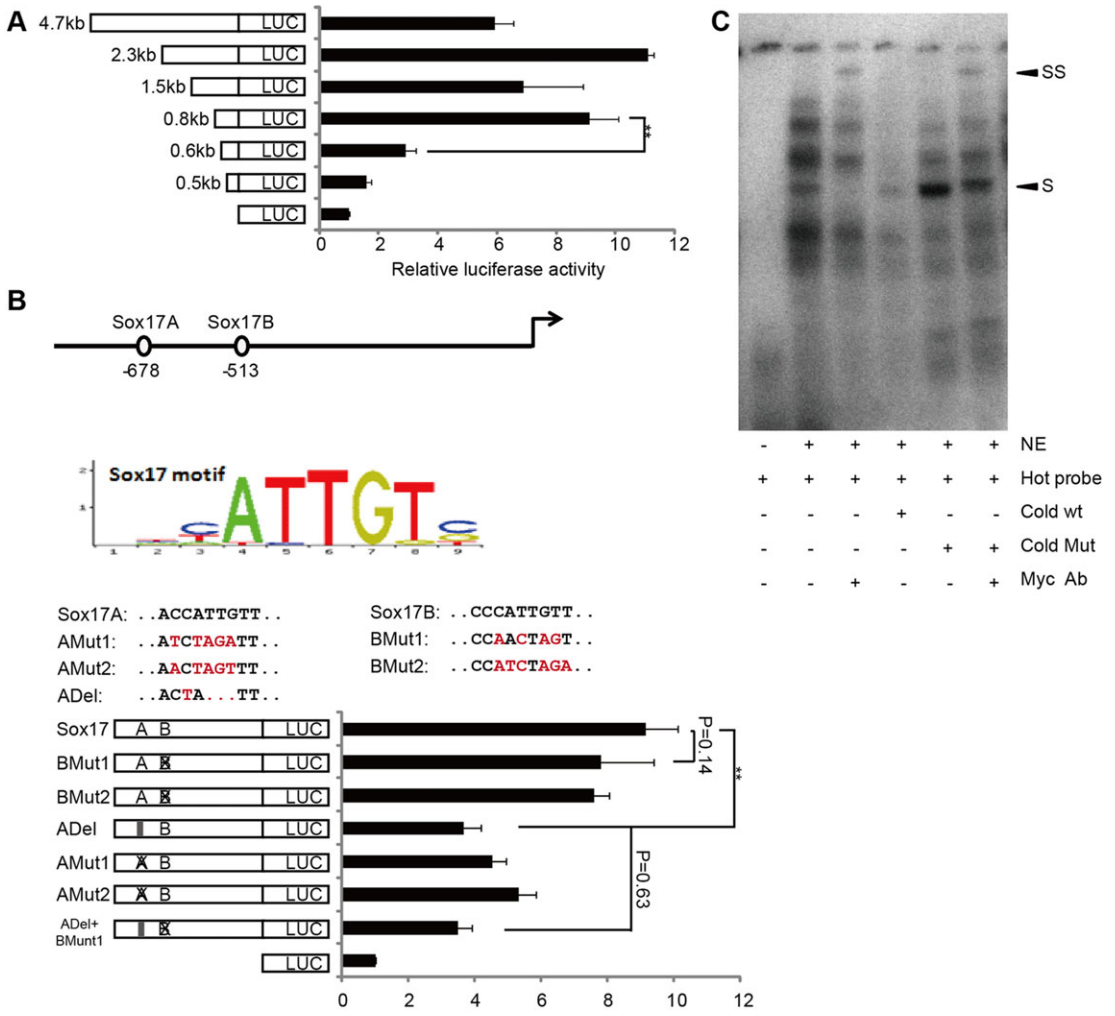

Fig. 2. Sox17 regulates the *Nepn* promoter through a direct binding site. (A) Luciferase constructs containing the *Nepn* transcriptional start site and upstream promoter regions were assayed in P19 cells co-transfected with either pBOS-Sox17 or pBOS-Venus. The length of the upstream region for each construct is indicated in the graphic. Relative luciferase activity represents the fold increase observed in the presence of ectopic Sox17 expression relative to vector control. (B) Schematic view of *Nepn* promoter indicating the two Sox17-binding sites and the consensus Sox17-binding motif from the JASPAR database. Mutations or deletions of either site A or site B in the 0.8 kb (842 bp) *Nepn* promoter luciferase vectors were generated, with mutations as indicated in red, and the vectors were tested in P19 cells. Relatively luciferase activity was determined as described above. (C) EMSA assay of nuclear protein binding to site A in the *Nepn* promoter. Myc-tagged Sox17 was ectopically expressed in HEK293T cells and nuclear extracts were incubated with ^{32}P-labeled Site A. Competition with a 100-fold excess of unlabeled wild-type or mutated Site A is indicated. Anti-Myc antibodies were included in the binding assay as indicated. S indicates the Sox17-Site A complex, SS indicates the super-shifted complex in the presence of anti-Myc antibody. ***P*<0.01. Mut, mutated; NE, nuclear extracts; wt, wild type.

luciferase activity of these constructs was evaluated in P19 cells in the presence of ectopically expressed *Sox17* (Fig. 2A). Constructs containing upstream regions with at least −842 bp and as much as −4.7 kb were induced 6- to 12-fold by *Sox17* expression. A significant drop in *Sox17*-inducible activity occurred when the sequence between −842 bp and −640 bp upstream of the *Nepn* TSS was deleted, suggesting that an enhancer region that is dependent on Sox17 lies in this region. To explore whether Sox17 regulates *Nepn* expression through direct binding on the *Nepn* promoter, we screened the *Nepn* upstream promoter region up to −842 bp for Sox17 DNA-binding motifs using the JASPAR database (Bryne et al., 2008). One potential binding site, site A, was identified at −678 bp and scored over 9 in JASPAR. We also observed a second high-scoring site, site B, at −513 bp. Conservation of these two sites is shown in supplementary material Fig. S1B. To evaluate the functionality of these sites, we generated mutations in the two putative binding sequences in the −842 bp promoter luciferase construct. Mutagenesis of site B did not affect the ability of Sox17 to induce the *Nepn* promoter, whereas either mutation or deletion of site A significantly decreased *Nepn* promoter activity in the presence of ectopic Sox17 expression (Fig. 2B). In addition, mutation of site B had little effect on the promoter activity when site A was deleted (Fig. 2B), suggesting that Sox17 induces *Nepn* expression through direct binding to site A. The ability of Sox17 to directly bind to site A was further confirmed by an electrophoretic mobility shift assay (EMSA) (Fig. 2C). Nuclear extracts from HEK293T cells ectopically expressing Myc-tagged Sox17 were incubated with radioactively labeled oligonucleotides containing site A. Several protein-DNA complexes were observed that were competitively reduced by both wild-type and mutated unlabeled binding sites, indicating non-Sox17-specific binding. One complex (S) was enhanced in the presence of unlabeled oligonucleotides containing a mutated Sox17-binding site and could be super-shifted with an anti-Myc antibody (SS), indicating that the complex contained Sox17 and the binding was specific (Fig. 2C). Together, our *in vivo* and *in vitro* data demonstrate that Sox17 positively

Development (2014) 141, 3772-3781 doi:10.1242/dev.108274

controls *Nepn* transcription within the midgut definitive endoderm through direct binding to the *Nepn* promoter region.

RA signaling enhances *Nepn* expression

Nepn is highly expressed in the midgut region of the embryo, but expression is absent in the foregut and hindgut pockets. As *Sox17* is expressed throughout the entire DE, additional factors must function to restrict the *Nepn* expression domain to the midgut. In the early mouse embryo, the RA-responsive domain, as shown using an RA response element (RARE)-*lacZ* reporter, is restricted to all three germ layers in the trunk region of the embryo (Rossant et al., 1991; Sakai et al., 2001; Mic et al., 2002), overlapping with expression of *Nepn*. Thus, we investigated whether RA signaling regulates *Nepn* expression by employing an *ex vivo* whole-embryo culture system, in which embryos were incubated in the presence of RA or the RA inhibitor BMS493. After culture for 24 h, embryos in the presence of BMS493 showed reduced expression of *Nepn* in a dosage-dependent manner (Fig. 3A-C). By contrast, *Nepn* expression was significantly upregulated in a dose-dependent manner in embryos cultured in the presence of exogenous RA for 24 h (Fig. 3D-G). Of note, the *Nepn* expression domain appears to extend further caudally in the presence of RA (arrow in Fig. 3E,F). To further confirm the role of RA in *Nepn* regulation, we analyzed *Nepn* expression in *Raldh2*$^{-/-}$ embryos (Mic et al., 2002). *Raldh2* (*Aldh1a2*) encodes retinaldehyde dehydrogenase 2 (Raldh2), which mediates an essential step in the synthesis of RA and is the primary homolog active in the gastrulating embryo (Duester, 2008). At E8.5, *Nepn* expression was drastically reduced in *Raldh2*$^{-/-}$ embryos, indicating that RA signaling is required for *Nepn* expression *in vivo* (Fig. 3H-K). In summary, *Nepn* expression is substantially decreased when RA signaling is reduced by deletion of *Raldh2* or inclusion of RA inhibitors, but upregulated with excess RA signaling.

As P19 is a characterized RA-responsive cell line, we tested whether RA is able to regulate *Nepn* expression in P19 cells. We found that endogenous *Nepn* expression was induced in P19 cells in a dosage-dependent manner (Fig. 4A). After 48 h of 0.1 μM RA treatment, *Nepn* expression was increased over 100-fold (Fig. 4B). Moreover, luciferase constructs containing the *Nepn* promoter region from the TSS to −8 kb upstream showed a strong activation in P19 cells treated with 0.1 μM RA (Fig. 4C). By using truncations of the −8 kb promoter to further localize the RA-responsive regions, we observed two dramatic drops in promoter activity, one between −2.3 kb and −0.6 kb upstream and the second between −0.3 kb and −0.5 kb upstream from the TSS (Fig. 4C). To investigate whether RA directly regulates *Nepn* expression, we analyzed the *Nepn* genomic region for RARE from the TSS to −8 kb with the JASPAR database. Four sites matching the RAR:RXR_DR5 consensus motif

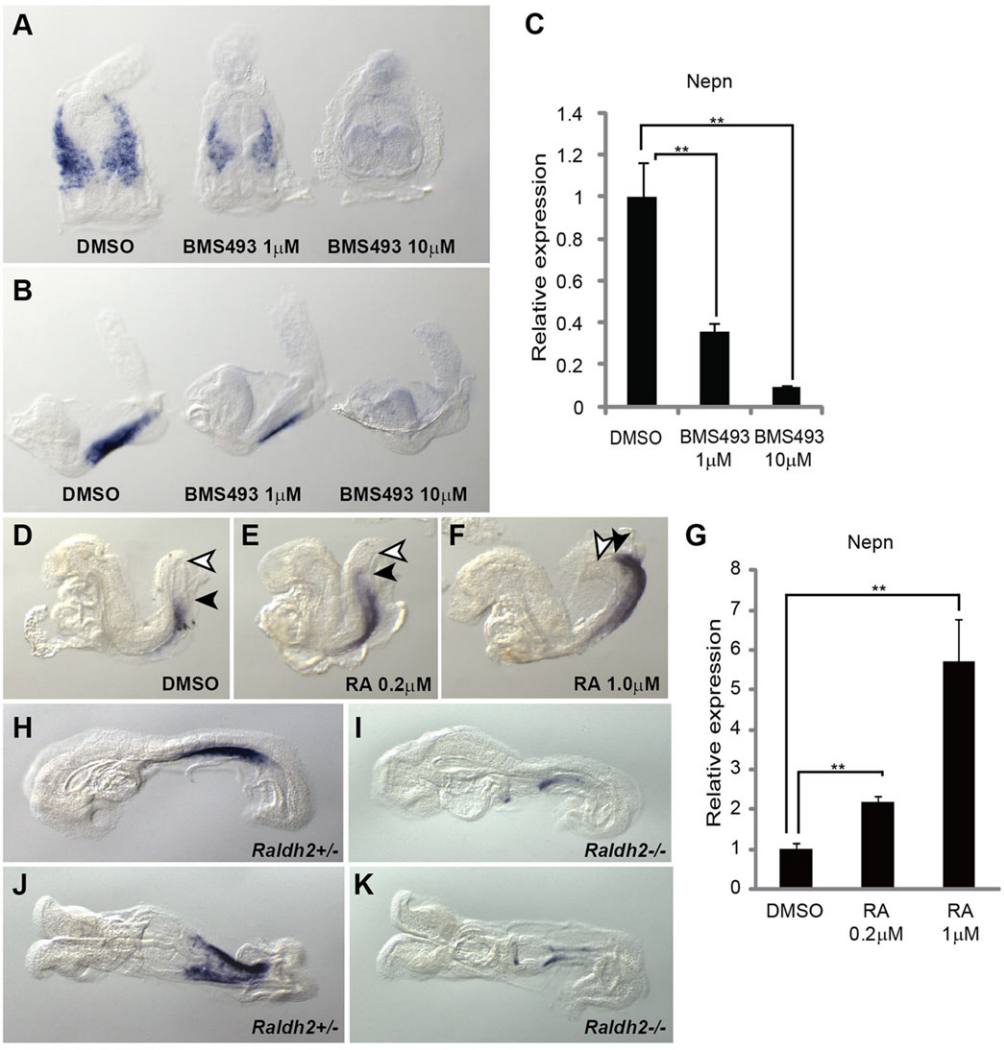

Fig. 3. RA signaling controls *Nepn* expression. (A,B) Posterior (A) and lateral (B) views of *Nepn* expression by WISH in embryos cultured for 24 h in either DMSO or the indicated concentration of BMS493, an RA inhibitor. (C) Quantitation of *Nepn* expression by RT-PCR of DMSO- and BMS493-treated embryos. Data obtained from three embryos were plotted. *Nepn* expression was reduced in the presence of BMS493. (D-F) Lateral views of *Nepn* expression by WISH in embryos cultured for 24 h in either DMSO or the indicated concentration of exogenous RA. Black arrowheads indicate the posterior boundary of *Nepn* domain; white arrowheads indicate the posterior end of the gut. For better comparison, these embryos were understained. (G) Quantitation of *Nepn* expression by RT-PCR of DMSO- and RA-treated embryos. Data obtained from three embryos were plotted. *Nepn* expression was increased in embryos cultured in the presence of RA. (H-K) Lateral (H,I) and ventral (J,K) views of *Nepn* expression in *Raldh2*$^{+/-}$ and *Raldh2*$^{-/-}$ embryos by WISH. *Nepn* was downregulated in *Raldh2*$^{-/-}$ embryos.

Development (2014) 141, 3772-3781 doi:10.1242/dev.108274

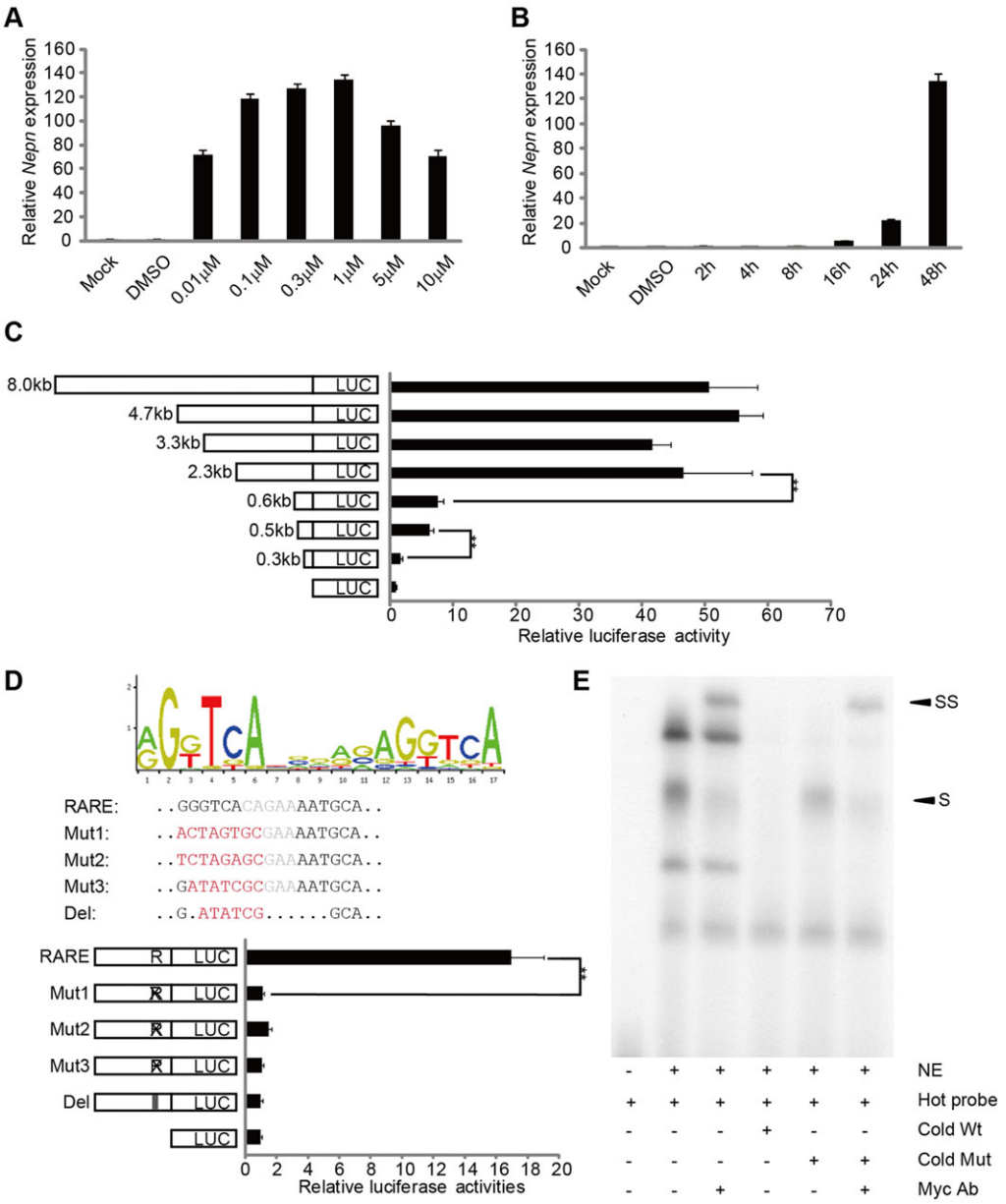

Fig. 4. RA signal directly regulates *Nepn* expression through an RARE. (A) P19 cells were treated with DMSO or RA for 48 h as indicated. Endogenous *Nepn* expression was measured by quantitative RT-PCR. (B) P19 cells were treated with DMSO or 0.1 μM RA as indicated. Endogenous *Nepn* expression was measured by quantitative RT-PCR. (C) Luciferase constructs containing the *Nepn* TSS and upstream promoter regions were assayed in P19 cells treated with DMSO or RA (0.1 μM). The length of the upstream region for each construct is indicated in the graphic. Relative luciferase activity represents the fold increase observed in the presence of RA relative to DMSO. (D) Consensus RARE (DR5) motif from the JASPAR database is shown with the sequence of the RARE from the *Nepn* promoter indicated below. Mutations or deletions of the *Nepn* RARE in the 2.3 kb *Nepn* promoter luciferase vectors were generated, with mutations as indicated in red, and the vectors were tested in P19 cells in the presence of DMSO or RA (0.1 μM). Relative luciferase activity was determined as described above. (E) EMSA assay of nuclear protein binding to the proposed RARE from the *Nepn* promoter. Myc-tagged RARα was ectopically expressed in P19 cells treated with RA (0.1 μM) and nuclear extracts were incubated with ^{32}P-labelled RARE from the *Nepn* promoter. Competition with a 100-fold excess of unlabeled wild-type or mutated RARE is indicated. Anti-Myc antibodies were included in the binding assay as indicated. S indicates the RARα-DNA complex; SS indicates the super shifted complex in the presence of anti-Myc antibody. ***P*<0.01. Mut, mutated; NE, nuclear extracts; Wt, wild type.

were identified. One of these sites, located at −381 bp upstream of the TSS, was highly conserved between several species by analysis using MULAN (Ovcharenko et al., 2005) (supplementary material Fig. S2A,B). This putative RARE consists of a canonical half site (GGGTCA) and a more diverse half site (AATGCA) separated by five nucleotides. Interestingly, mutation of this site within the −2.3 kb construct abolished the promoter's ability to respond to RA signaling (Fig. 4D), suggesting that this site is crucial for *Nepn* expression. We further confirmed direct binding of the RA receptor, RARα, with the DNA sequence of this region through EMSA, in which we expressed Myc-tagged RARα in P19 cells. Together, these results indicate that RA signaling directly regulates *Nepn* expression through a RARE located at −381 bp.

Given that both Sox17 and RA can directly regulate *Nepn* expression, we next explored whether Sox17 and RA regulate *Nepn* expression in a cooperative fashion. Sox17 or tSox17 (Kanai et al., 1996) were ectopically expressed in P19 cells in the presence of RA or DMSO. Indeed, combination of ectopic *Sox17* expression and RA increased endogenous *Nepn* expression approximately twofold over either factor alone (Fig. 5B). Moreover, luciferase assays indicated that promoter activity of the construct (2.3 kb) that contains both Sox17-binding motif and RARE was dramatically enhanced with ectopic expression of *Sox17* in the presence of RA. Mutation of either the Sox17 DNA-binding site or the RARE significantly reduced this synergistic effect (Fig. 5C). Together, Sox17 and RA cooperate to promote *Nepn* expression.

To evaluate whether the *Nepn* promoter containing the Sox17-binding site and RARE is sufficient to drive midgut DE expression *in vivo*, we generated transient transgenic embryos using a *lacZ* reporter gene driven by the 2.3 kb *Nepn* promoter. Strong *lacZ* staining was observed in the definitive endoderm in E7.5-8.5 transgenic embryos (four out of four) (Fig. 5D-G), overlapping with the *Nepn* expression domain (Hou et al., 2007). Of note, although the expression did not extend into the foregut region, expression in the hindgut was observed in two of the embryos that showed strong *lacZ* staining (Fig. 5D,E), suggesting that both Sox17 and RA

Development (2014) 141, 3772-3781 doi:10.1242/dev.108274

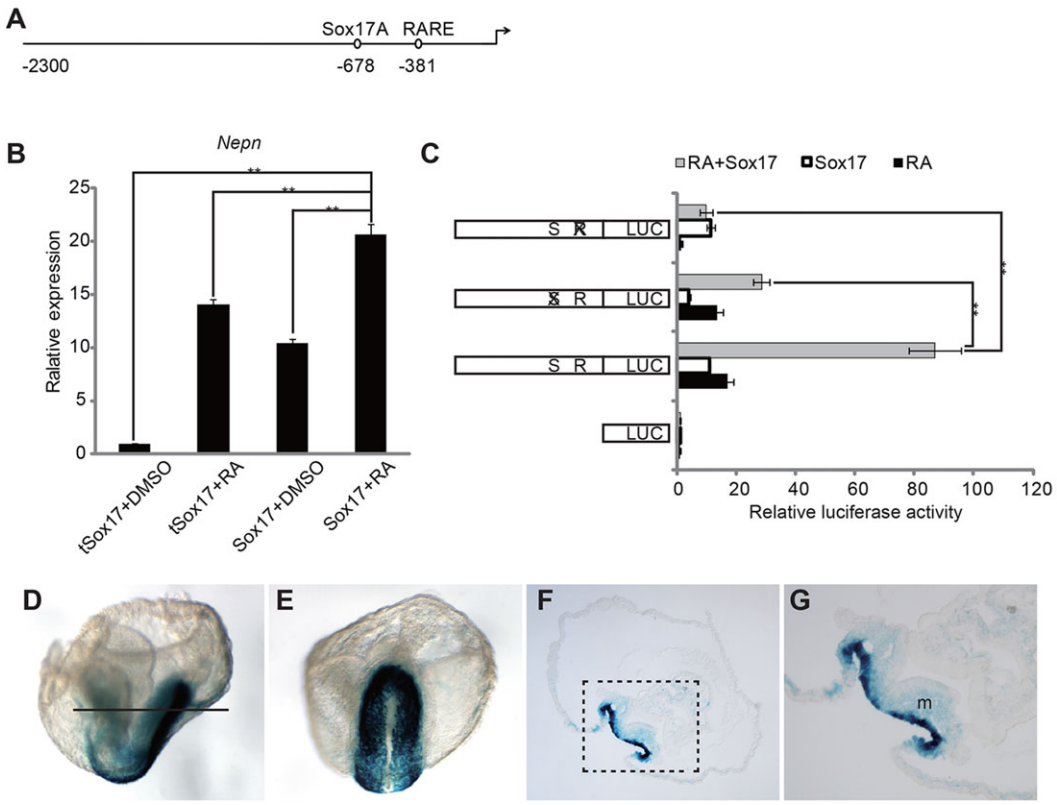

Fig. 5. RA signaling and Sox17 cooperate to enhance *Nepn* expression. (A) Schematic view of *Nepn* promoter indicating the Sox17-binding site and RARE. (B) P19 cells were transfected with pBOS-Sox17 or pBOS-tSox17 and cultured in the presence of DMSO (0.1%) or RA (0.1 μM). Endogenous *Nepn* expression was measured by quantitative RT-PCR. (C) P19 cells were co-transfected with the 2.3 kb *Nepn* promoter luciferase vector that was either unmodified or mutated in the Sox17 Site A or the *Nepn* RARE, as indicated, and with pBOS-Sox17 in the presence of DMSO, pBOS-Sox17 in the presence of RA or pBOS-Venus in the presence of RA or DMSO. The gray bars indicate fold change in relative luciferase activity of *Nepn* promoter within cells transfected with pBOS-Sox17 and treated with RA relative to cells transfected with pBOS-Venus and treated with DMSO; the white bars indicate the fold change of cells transfected with pBOS-Sox17 to cells with pBOS-venus; the black bars indicate the fold change of cells treated with RA to cells treated with DMSO. *Sox17* expression and RA synergize to activate the *Nepn* promoter. ***P*<0.01. (D,E) Lateral view (D) and posterior view (E) of whole-mount *lacZ* staining of somite 5 embryo. A cross section (indicated by the line) of the embryo in D is shown in F and G. The DE shows strong *lacZ* staining, whereas mesoderm has weak staining. m, mesoderm.

signaling can regulate gene expression in the hindgut *in vivo*. Thus, additional elements are likely required to refine the posterior boundary. Low levels of *lacZ* expression were also detected in mesoderm (three out of four embryos) (Fig. 5F), suggesting that the 2.3 kb promoter region is able to weakly respond to RA signaling in mesoderm. Together, our results support a model in which Sox17 and RA are required for expression of *Nepn* in midgut definitive endoderm.

The anterior *Nepn* expression boundary is dependent on Nodal signaling

Nodal signaling is essential for DE formation. Removal of maternal RA by embryonic Cyp26 (Cyp26a1b1/c1 – Mouse Genome Informatics)-mediated RA degradation has been shown to be necessary to correctly regulate *Nodal* expression in the embryo (Uehara et al., 2009). To explore whether Nodal signaling regulates *Nepn* expression, we examined RA-dependent induction of endogenous *Nepn* in P19 cells in the presence and absence of exogenous ActivinA. In these studies, we used ActivinA as a ligand, as it activates the same receptor, ALK4 (also known as Acvr1b), and intracellular signaling pathways as Nodal without a requirement for a co-receptor (e.g. Cripto). In P19 cells, ActivinA alone did not induce *Nepn* expression (supplementary material Fig. S3A). However, *Nepn* expression demonstrated a concentration-dependent response to addition of ActivinA in the presence of RA. ActivinA at low concentrations (5-10 ng/ml) strongly synergized with RA and induced *Nepn* expression nearly 300-fold. By contrast, ActivinA at a high concentration (100 ng/ml), which is commonly used for endoderm differentiation of stem cells, inhibited RA-dependent induction of *Nepn* (Fig. 6A). As RA is able to induce Sox17 in F9, an embryonic carcinoma cell line (Futaki et al., 2003), we examined whether induction of *Sox17* was responsible for the dose-dependent response of *Nepn* to RA and ActivinA in P19 cells. Of note, *Sox17* was induced by RA in P19 cells, but its expression was not varied by addition of low amounts of ActivinA (1-20 ng/ml) (Fig. 6A), indicating that the mechanism of synergistic activity of low Activin with RA is not through increased expression of *Sox17*.

We next examined if the Nodal/Activin signaling pathway alters the *Nepn* expression domain *in vivo* by examining *Foxh1*$^{-/-}$ embryos. Foxh1 is a transcription factor that mediates high levels of Nodal signaling during gastrulation through an auto-regulatory loop (Saijoh et al., 2000; Norris et al., 2002). Loss of *Foxh1* results in a failure to form foregut endoderm, whereas midgut endoderm is evident (McKnight et al., 2010). This phenotype is similar to mice carrying a deletion in the Foxh1-dependent auto-regulatory enhancer in *Nodal* (Norris et al., 2002). To determine whether reduced Nodal signaling affected *Nepn* expression, we examined E8.5-9.5 *Foxh1*$^{-/-}$ embryos (Fig. 6B). In embryos in which morphogenesis is less severely disrupted (Hoodless et al., 2001; Yamamoto et al., 2001), we observed that the *Nepn* expression

Development (2014) 141, 3772-3781 doi:10.1242/dev.108274

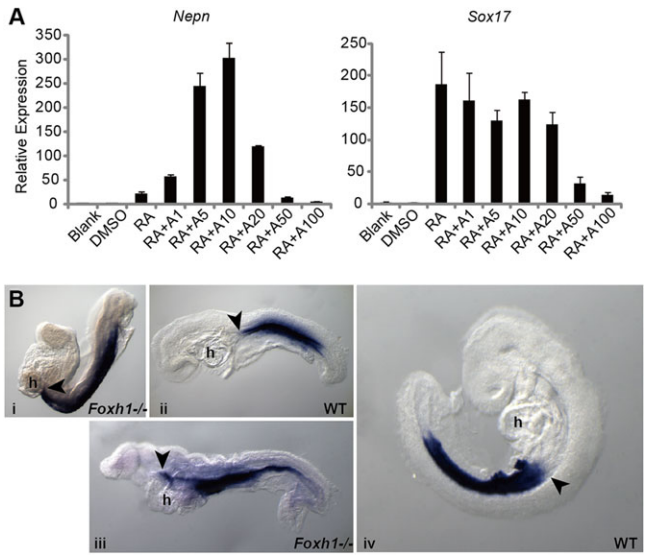

Fig. 6. The *Nepn* expression domain is expanded anteriorly in *Foxh1*$^{-/-}$ embryos. (A) P19 cells were cultured in reduced serum (1% FBS) in the presence of RA (0.1 μM) in combination with increasing doses of ActivinA as indicated (in ng/ml) for 48 h. Endogenous *Nepn* (left) and *Sox17* (right) expressions were quantified by RT-PCR. Total RNA was extracted 48 h after each treatment. (B) WISH for Nepn expression in *Foxh1*$^{-/-}$ embryos at E8.5 (i,ii) and E9.5 (iii,iv) (lateral views shown). A representative image of mutants is shown at each stage. *Nepn* expression was upregulated in *Foxh1*$^{-/-}$ embryos, which exhibited an anterior extension of *Nepn* domain. Black arrowheads indicate the anterior boundary of *Nepn*. h, heart; WT, wild type.

domain was expanded into the anterior gut region. In wild-type embryos, *Nepn* expression is always posterior to the heart and anterior intestinal portal (AIP), whereas in *Foxh1*$^{-/-}$ embryos, *Nepn* expression extends anteriorly, dorsal to the heart (arrow in Fig. 6B), suggesting that high levels of Nodal signaling define the anterior boundary by inhibiting midgut marker *Nepn* expression. Together, our data suggest that Nodal/Activin signaling can modulate RA-dependent *Nepn* expression.

DISCUSSION

The mechanisms that define developmental domains and in particular the boundaries that limit those domains is crucial to understanding organogenesis in the embryo. Multiple signaling pathways have been implicated in endoderm patterning, including Nodal, RA, Wnt and FGF. Much of our understanding has been developed from *in vitro* studies of human and mouse stem cell differentiation. How these pathways interact *in vivo* is less well understood. Moreover, given the lack of DE-domain-specific markers, most of the work on DE patterning has been done using organ-specific markers that turned on at later stages of organogenesis (Wendling et al., 2000; Chen et al., 2007; Bayha et al., 2009). We previously identified *Nepn* as a unique, specific marker of midgut DE (Hou et al., 2007). Its expression initiates at E7.25, before overt formation of midgut endoderm, suggesting that midgut patterning begins early in development. Thus, *Nepn* provides a valuable tool to study early midgut patterning mechanisms, before organogenesis. Here, using a combination of *in vivo*, *ex vivo* and *in vitro* approaches, we identified two regulatory elements in the upstream promoter regions of *Nepn*: one at −381 bp is an RARE and a second at −678 bp is responsive to direct binding of Sox17. We observed that Sox17 and RA can cooperate to significantly increase *Nepn* promoter activity *in vitro* and that this promoter region can direct strong *lacZ* expression to DE *in vivo*. Furthermore, *Nepn* expression is tightly regulated by Nodal/Activin A signaling, with high levels inhibiting its expression and low levels enhancing its expression. Our data further support the idea that the level of Activin/Nodal signaling is crucial to define the anterior boundary of *Nepn* expression *in vivo*. Together, these signaling pathways and transcription factors form a network that regulates *Nepn* expression and defines the midgut domain.

Nepn expression is directly regulated by Sox17 and RA signaling

The transcription factor Sox17 functions as an endoderm determinant (Kanai-Azuma et al., 2002). Embryos lacking Sox17 exhibit reduced DE in the mid- and hindgut and Sox17-null embryonic stem cells are completely excluded from the mid- and hindgut in chimera assays, demonstrating the essential role of Sox17 in mid- and hindgut patterning (Kanai-Azuma et al., 2002). Consistent with the lack of midgut and hindgut, *Nepn* is absent in *Sox17*$^{-/-}$ embryos at E8.5. Moreover, our data indicate that *Nepn* is also a direct target of Sox17. Of note, by E9.0, weak expression of *Nepn* is observed in *Sox17*$^{-/-}$ embryos (Fig. 1Avi), suggesting that Sox17 is not essential at this stage. As Sox9 is able to induce *Nepn* in MEL cells (supplementary material Fig. S4), it may be compensating for the loss of Sox17. Interestingly, in β-catenin (Ctnnb1 – Mouse Genome Informatics) conditional knockout embryos in which Sox17 is almost absent, *Nepn* expression was also substantially decreased (Engert et al., 2013), suggesting that Wnt/β-catenin indirectly regulates *Nepn* expression through Sox17.

As *Sox17* is more broadly expressed than *Nepn*, including in the visceral endoderm and throughout the foregut, midgut and hindgut (Kanai-Azuma et al., 2002), factors in addition to Sox17 are required to control *Nepn* expression in the midgut. We found that RA signaling is a potent inducer of *Nepn* expression and it is dramatically reduced in *Raldh2*$^{-/-}$ embryos, confirming its dependence on RA. Moreover, we observed that RA signaling can cooperate with Sox17 in P19 cells. *Nepn* is directly regulated by RA through a responsive element that is able to bind RARα. Of note, in P19 cells, *Nepn* expression is dramatically increased with relatively low concentrations of RA (0.1 μM), suggesting that *Nepn* promoter is highly sensitive to RA signaling. However, *Nepn* expression is not significantly upregulated until after 16 h of RA treatment in P19 cells, implying that induction of additional co-regulators, such as Sox17, are required. Notably, the 2.3 kb promoter region of *Nepn*, which contains the Sox17-binding site and the RARE, is sufficient to drive gene expression in the DE of transgenic embryos.

Nepn is first expressed at E7.25 in the mouse embryo and by E8.0, *Nepn* is expressed in the lateral DE. By E10.5, *Nepn* is expressed caudally from the stomach throughout dorsal pancreas and intestine (Hou et al., 2007), encompassing the *Pdx1* expression domain (supplementary material Fig. S5). By E11.5, the expression of *Nepn* and *Pdx1* substantially overlap, although the expression of *Nepn* in the ventral pancreatic bud is substantially weaker compared with its expression in the dorsal pancreatic bud (supplementary material Fig. S5). By E14.5, Nepn is restricted to the exocrine pancreas (Anderson et al., 2009). Most recently, *Nepn* was found to label pancreatic progenitors in embryonic stem cell differentiation (De Angelis et al., 2014). Previous studies have shown that Sox17 function is essential for *Pdx1* expression in the dorsal and ventral pancreatic primordial (Kanai-Azuma et al., 2002). In those studies, *Hex* expression was normal in *Sox17*$^{-/-}$ embryos, indicating that liver and thyroid primordia are formed. Moreover, development of the dorsal pancreatic bud was absent in *Raldh2*$^{-/-}$ embryos (Martin et al., 2005; Molotkov et al., 2005). In these mutants, *Pdx1* was

Development (2014) 141, 3772-3781 doi:10.1242/dev.108274

expressed in the ventral pancreatic bud but was absent in the dorsal pancreatic region. Thus, *Nepn* and *Pdx1* expression share several common regulatory mechanisms *in vivo*, although *Nepn* is expressed substantially earlier than *Pdx1*. Together, the regulation of *Nepn* by Sox17 and RA signaling supports a crucial role for these factors in the patterning of the midgut DE.

RA and Activin/Nodal signaling define the boundaries of *Nepn* expression

Based on a *RARE-lacZ* reporter transgenic mouse line, the region responsive to RA signaling is localized to the trunk region of the embryo, posterior to the preotic sulcus, with lower levels of RA responsiveness extending into the hindgut (Sirbu and Duester, 2006). The limits of the domain are regulated by a balance between the synthesis and metabolism of RA. Raldh2, the primary enzyme that synthesizes RA in the embryo, is not present in the DE but is found in the adjacent mesoderm. *Raldh2* expression in the trunk mesoderm extends from the anterior region of the tailbud to the level of the posterior foregut (Molotkov et al., 2005). *Cyp26a1* encodes an RA-metabolizing enzyme and is expressed in the head and posterior region of the tailbud, thus restricting high RA activity to the trunk (Abu-Abed et al., 2001; Sakai et al., 2001; Sirbu et al., 2005). *In vivo*, *Nepn* is exclusively expressed in the DE, and the anterior and posterior boundaries of *Nepn* are similar to those of the high RA-responsive domain in the trunk of the embryo, hinting that RA signaling may modulate the anterior and posterior boundaries of *Nepn* expression. A recent study in chick embryos showed that organogenesis in the entire endoderm is patterned along anteroposterior axis through RA signaling, in particular by regulating *CdxA* (Bayha et al., 2009). In our transgenic embryos, although the anterior boundary is maintained, the 2.3 kb promoter region of *Nepn* that contains the Sox17-binding site and the RARE is sufficient to drive *lacZ* expression throughout the hindgut region, suggesting that the posterior boundary is not maintained. It is possible that the *Nepn* promoter is highly sensitive to RA and is responding to the lower levels of RA in the hindgut region. Together, our results support a model in which Sox17 restricts *Nepn* expression to the DE while RA signaling promotes expression in the midgut and hindgut. Additional factors, possibly Cdx related, are probably necessary to refine the posterior boundary of *Nepn* expression (Fig. 7).

As high levels of Nodal are required for foregut formation, we examined *Foxh1*$^{-/-}$ embryos in which Nodal signaling is reduced and foregut formation is disrupted (McKnight et al., 2010). In *Foxh1*$^{-/-}$ embryos, *Nepn* expression extends into the anterior pocket region, indicating that *Nepn* expression can be expressed anterior to the anterior intestinal portal and suggesting that the foregut region in these embryos has a midgut identity. We further observed that *Nepn* expression can be controlled in P19 cells by Activin in a dose-dependent manner, in conjunction with RA. At high Activin concentrations normally used for endoderm induction in stem cells (100 ng/ml), RA-dependent induction of *Nepn* is inhibited; at lower doses of Activin (10 ng/ml), *Nepn* expression is significantly enhanced. We were not able to identify an Activin response element in the *Nepn* promoter, although one could be outside of the domain studied here (supplementary material Fig. S3B). Alternatively, Activin may indirectly enhance *Nepn* RA-dependent expression, as Activin may promote differentiation of the P19 cells. Although the levels of *Sox17* were not affected by inclusion of Activin, *Nepn* expression in response to Activin and RA correlates with the expression of *Cdx2* in P19 cells (supplementary material Fig. S6A), suggesting that at the lower concentrations of Activin, P19 cells have a posterior identity. Of note, *Nepn* expression is absent in *Cdx1*$^{-/-}$;*Cdx2*$^{-/-}$ embryos (supplementary material Fig. S6B), indicating that midgut endoderm is not formed and supporting studies showing that in the absence of *Cdx2*, the endoderm is converted to foregut/esophageal-like cells (Gao et al., 2009). Of interest, we were not able to identify an Activin responsive element in luciferase assays using the 8 kb promoter region upstream of *Nepn*, suggesting that the Activin regulatory region lies outside of the region analyzed. Alternatively, *Nepn* induction by Activin may be indirect by promoting differentiation of the cells to foregut endoderm and establishing the anterior boundary through regulation of RA signaling.

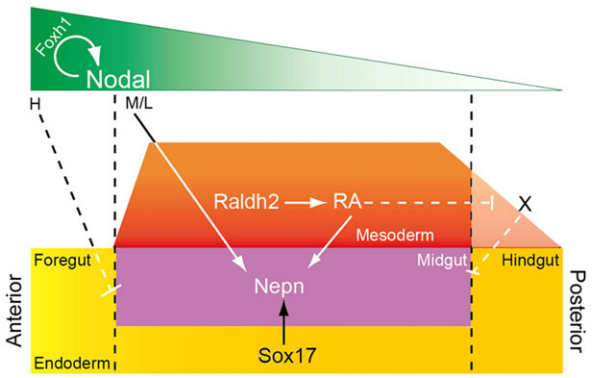

Fig. 7. Pathway interactions regulating midgut patterning. During gastrulation, Nodal establishes a morphogen gradient to specify nascent endoderm from primitive streak. The Foxh1-mediated high Nodal signal (H) is crucial for foregut patterning and the establishment of foregut-midgut boundary; medium/low (M/L) amount of Nodal enhances *Nepn* expression. The expression of Sox17 restricts *Nepn* expression domain to the DE. RA is secreted from the adjacent mesoderm and diffuses to the endoderm to further restrict *Nepn* expression in the midgut region. Higher RA signaling facilitates the expansion of *Nepn* expression domain posteriorly.

Nepn is a member of the small leucine-rich repeat (SLRP) family of proteins. It is a secreted, N-glycosylated inhibitor of TGFβ signaling (Mochida et al., 2006) and a potent inhibitor of Activin signaling (supplementary material Fig. S7). Due to the similarities between Nodal and Activin signaling, it is possible that *Nepn* can also inhibit Nodal signaling in the embryo. Moreover, *Nodal* has an RA-responsive element and can be ectopically induced in E6.5 embryos lacking all three *Cyp26* genes that fail to degrade RA derived from the maternal bloodstream (Uehara et al., 2009); embryonic RA synthesis does not begin until E7.5 when *Raldh2* expression is first observed (Sirbu et al., 2005). Thus, RA does not normally interfere with Foxh1 function to properly induce high levels of Nodal to promote foregut formation. As development proceeds, Nepn may be induced by RA to inhibit Nodal signaling and prevent posterior expansion of the foregut domain in the DE. As high levels of Nodal signaling are required for foregut, but not midgut or hindgut formation, the balance between foregut and midgut could be altered by RA signaling. Thus, our data suggest that Nodal, RA and Nepn may form a feedback loop to regulate the foregut-midgut boundary in the embryo (Fig. 7). Further studies to explore the relationship of these factors will be required.

In summary, our data support a model in which a core regulatory network comprised of Nodal/Activin signaling, RA signaling and Sox17 regulate *Nepn* expression and pattern the midgut DE. In this core network, Sox17 is required for *Nepn* expression in DE. RA synthesized from adjacent mesoderm cells, diffuses to regulate *Nepn* expression within the midgut domain and, along with an

Development (2014) 141, 3772-3781 doi:10.1242/dev.108274

unknown factor, contribute to the posterior boundary. The *Nepn* anterior boundary is refined by a feedback loop formed by Nepn, RA and Nodal/Activin signaling (Fig. 7). Our work supports and extends previous models (Zorn and Wells, 2009; Kraus and Grapin-Botton, 2012) with *in vivo* molecular data in the mouse. Moreover, other signaling pathways, such as Wnt and FGF, are involved in both endoderm formation and patterning and are likely to contribute to *Nepn* regulation.

MATERIALS AND METHODS

Whole-mount *in situ* hybridization (WISH)

All mouse studies conformed to the regulatory standards and protocols adopted by the appropriate animal oversight committees at the University of British Columbia, University of Utah, Sanford–Burnham Medical Research Institute, University of Ottawa or McGill University Animal Research Committee at the Sanford–Burnham Medical Research Institute. Embryos were obtained from crosses of *Foxh1* (Hoodless et al., 2001), *Sox17* (Saund et al., 2012) or *Raldh2* (Mic et al., 2002) heterozygous mice. Embryos were staged based on morphology and the number of somites, as previously described (Downs and Davies, 1993). Embryos were dissected from the uterus in DPBS (Invitrogen), fixed with 4% paraformaldehyde overnight at 4°C, dehydrated through a graded methanol series and stored at −20°C. WISH was carried out as previously described (Hou et al., 2007). Staged-matched heterozygous littermates were used as controls. For each experiment, at least five embryos were examined, and representative embryos are shown in the figures. The *Nepn in situ* probe was previously described (Hou et al., 2007).

Cell culture, vector construction and luciferase reporter assay

P19 and MEL cells were cultured in DMEM (STEMCELL Technologies) supplemented with 10% FBS (Hyclone). RA was reconstituted in DMSO to a working stock of 10^{-3} M. Corresponding amounts of DMSO were supplemented as a control in all experiments. *Nepn* upstream regions were generated by PCR from bacterial artificial clone (BAC) DNA, RP24-251C12, and cloned into pGL3 basic luciferase reporter vector (Promega). Reporter vectors were co-transfected with the *Renilla* luciferase construct, TK-RL, and, if indicated, with pBOS-Sox17 or pBOS-Venus. P19 cells were seeded at 5×10^4/well in a 24-well plate and transfected with Lipofectamine 2000 (Invitrogen) according to the manufacturer's instructions. For each well, 0.8 µg of the reporter luciferase vector, 0.02 µg TK-RL and 0.04 µg Sox17 or control vector were typically used. The medium was refreshed with indicated treatments 6 h after transfection. Cell lysates were collected 48 h after transfection, and Firefly and *Renilla* luciferase activities were measured using the Dual Luciferase Assay (Promega) according to the manufacturer's instructions. Firefly luciferase was normalized to *Renilla* luciferase, and normalized to the respective negative controls (DMSO or pBOS-Venus).

Transient transgenic reporter assay

To construct the *lacZ* reporter vector, *lacZ* was subcloned into pGL3 to replace firefly luciferase. The microinjection and *lacZ* staining were performed as previously described (Uehara et al., 2009; Yamanaka et al., 2010).

RNA quantification

Total RNA was extracted with Trizol (Invitrogen) using MaXtracthigh density phase-lock gels (Qiagen). RNA was reverse-transcribed and quantified using SYBR Green-based real-time PCR (qRT-PCR) according to manufacturer's instructions (Roche) with ABI PRISM 7300 Sequence Detection System. *Gapdh* or *actin* served as controls for normalization.

Whole-embryo culture

E7.5 Institute of Cancer Research (ICR) mouse embryos were dissected in warm DMEM supplemented with 10% FBS. Embryos with similar developmental stage were transferred to 50 ml falcon tubes containing 50% rat serum in DMEM in the presence of either RA, BMS493 or DMSO, and rotated for 24 h under 5% CO_2 at 37°C as described (Yamamoto et al., 2003). For each condition, at least five embryos were examined, and representative embryos are shown.

Electrophoretic mobility supershift assay

Myc-Sox17 and Myc-RARα were generated from pBOS-Sox17, which was cloned from mouse cDNA (Kanai et al., 1996) and pSG5-RARα (Underhill et al., 1994), respectively, by subcloning into the vector N′ Myc-V517 (Turkson et al., 2004; Colwill et al., 2006). For Sox17 binding assay, cell nuclear extracts were prepared from HEK293T cells with V518-Myc-Sox17. For RARα binding assay, cell nuclear extracts were prepared from RA-treated P19 cells transfected with V518-Myc-RARα. Wild-type or mutant oligos containing transcription factor-binding sites were annealed with their antisense. Then, double-stranded wild-type oligonucleotides were radiolabeled with (γ-^{32}P) ATP using T4 polynucleotide kinase according to the manufacturer's instructions (Invitrogen). Gel shift assays were performed as previously described using Novex EMSA gel system (Invitrogen) (Xiang et al., 2010). Anti-Myc antibody was purchased from Covance.

Statistics

All data presented are representative of at least three independent experiments unless indicated otherwise. Data are presented as mean±s.d. Statistical analysis was performed using Student's *t*-test. Statistical significance was inferred at $*P<0.05$ and $**P<0.01$.

Acknowledgements

We thank Dr Masami and Yoshi Kanai for Sox17 and tSox17 expression vector, Dr Michael Underhill for kindly sharing pSG5-RARα, and Dr Se-Wing Grace Cheng and Dr Gregg B. Morin for N′ V517-Myc.

Competing interests

The authors declare no competing financial interests.

Author contributions

J.H., W.W., Yu.Y., D.Y.D.L., O.A., N.A.J.K., R.M., R.C. and N.H. performed experimental procedures under the guidance of P.A.H. J.H. performed the embryo culture, luciferase assay and analyzed the *Foxh1* mutant. W.W. performed the cell culture experiments and molecular cloning. D.Y.D.L., N.A.J.K., R.M. and R.C. performed quantitative RT-PCR assay. P.X., O.A. and R.K.H. performed EMSA assay. R.S.S. and Y.S. analyzed the *Sox17* mutant; T.J.C. and G.D. analyzed the *Raldh2* mutant; J.G.A.S. and D.L. analyzed the double mutant of *Cdx1* and *Cdx2*; N.H. and Yo.Y. performed transient transgenic assay. J.H., W.W. and P.A.H. wrote the manuscript.

Funding

This work was supported by funding from the Canadian Institute of Health Research [FRN 89806 to P.A.H.]; the Natural Sciences and Engineering Research Council of Canada [RGPIN 418298-12 to P.A.H., RGPIN 418720-12 to Yo.Y.]; and National Institutes of Health grants [R01HD0066121 to Y.S., GM062848 to G.D.]. Deposited in PMC for release after 12 months.

Supplementary material

Supplementary material available online at
http://dev.biologists.org/lookup/suppl/doi:10.1242/dev.108274/-/DC1

References

Abu-Abed, S., Dollé, P., Metzger, D., Beckett, B., Chambon, P. and Petkovich, M. (2001). The retinoic acid-metabolizing enzyme, CYP26A1, is essential for normal hindbrain patterning, vertebral identity, and development of posterior structures. *Genes Dev.* **15**, 226-240.

Anderson, K. R., White, P., Kaestner, K. H. and Sussel, L. (2009). Identification of known and novel pancreas genes expressed downstream of Nkx2.2 during development. *BMC Dev. Biol.* **9**, 65.

Arnold, S. J., Hofmann, U. K., Bikoff, E. K. and Robertson, E. J. (2008). Pivotal roles for eomesodermin during axis formation, epithelium-to-mesenchyme transition and endoderm specification in the mouse. *Development* **135**, 501-511.

Bayha, E., Jørgensen, M. C., Serup, P. and Grapin-Botton, A. (2009). Retinoic acid signaling organizes endodermal organ specification along the entire antero-posterior axis. *PLoS ONE* **4**, e5845.

Bryne, J. C., Valen, E., Tang, M.-H. E., Marstrand, T., Winther, O., da Piedade, I., Krogh, A., Lenhard, B. and Sandelin, A. (2008). JASPAR, the open access database of transcription factor-binding profiles: new content and tools in the 2008 update. *Nucleic Acids Res.* **36**, D102-D106.

Development (2014) 141, 3772-3781 doi:10.1242/dev.108274

Chen, Y., Pan, F. C., Brandes, N., Afelik, S., Sölter, M. and Pieler, T. (2004). Retinoic acid signaling is essential for pancreas development and promotes endocrine at the expense of exocrine cell differentiation in Xenopus. *Dev. Biol.* **271**, 144-160.

Chen, F., Desai, T. J., Qian, J., Niederreither, K., Lu, J. and Cardoso, W. V. (2007). Inhibition of Tgf beta signaling by endogenous retinoic acid is essential for primary lung bud induction. *Development* **134**, 2969-2979.

Colwill, K., Wells, C. D., Elder, K., Goudreault, M., Hersi, K., Kulkarni, S., Hardy, W. R., Pawson, T. and Morin, G. B. (2006). Modification of the Creator recombination system for proteomics applications–improved expression by addition of splice sites. *BMC Biotechnol.* **6**, 13.

De Angelis, M. T., Russo, F., D'Angelo, F., Federico, A., Gemei, M., Del Vecchio, L., Ceccarelli, M., De Felice, M. and Falco, G. (2014). Novel Pancreas Organogenesis Markers Refine the Pancreatic Differentiation Roadmap of Embryonic Stem cells. *Stem Cell Rev.* **10**, 269-279.

Dessimoz, J., Opoka, R., Kordich, J. J., Grapin-Botton, A. and Wells, J. M. (2006). FGF signaling is necessary for establishing gut tube domains along the anterior-posterior axis in vivo. *Mech. Dev.* **123**, 42-55.

Downs, K. M. and Davies, T. (1993). Staging of gastrulating mouse embryos by morphological landmarks in the dissecting microscope. *Development* **118**, 1255-1266.

Duester, G. (2008). Retinoic acid synthesis and signaling during early organogenesis. *Cell* **134**, 921-931.

Dufort, D., Schwartz, L., Harpal, K. and Rossant, J. (1998). The transcription factor HNF3beta is required in visceral endoderm for normal primitive streak morphogenesis. *Development* **125**, 3015-3025.

Engert, S., Burtscher, I., Liao, W. P., Dulev, S., Schotta, G. and Lickert, H. (2013). Wnt/beta-catenin signalling regulates Sox17 expression and is essential for organizer and endoderm formation in the mouse. *Development* **140**, 3128-3138.

Futaki, S., Hayashi, Y., Yamashita, M., Yagi, K., Bono, H., Hayashizaki, Y., Okazaki, Y. and Sekiguchi, K. (2003). Molecular basis of constitutive production of basement membrane components: gene expression profiles of Engelbreth-Holm-Swarm tumor and F9 embryonal carcinoma cells. *J. Biol. Chem.* **278**, 50691-50701.

Gao, N., White, P. and Kaestner, K. H. (2009). Establishment of intestinal identity and epithelial-mesenchymal signaling by Cdx2. *Dev. Cell* **16**, 588-599.

Goessling, W., North, T. E., Lord, A. M., Ceol, C., Lee, S., Weidinger, G., Bourque, C., Strijbosch, R., Haramis, A.-P., Puder, M. et al. (2008). APC mutant zebrafish uncover a changing temporal requirement for wnt signaling in liver development. *Dev. Biol.* **320**, 161-174.

Grapin-Botton, A. (2008). *Endoderm Specification StemBook*. Cambridge, MA: Harvard Stem Cell Institute.

Gregorieff, A., Grosschedl, R. and Clevers, H. (2004). Hindgut defects and transformation of the gastro-intestinal tract in Tcf4(–/–)/Tcf1(–/–) embryos. *EMBO J.* **23**, 1825-1833.

Hoodless, P. A., Pye, M., Chazaud, C., Labbé, E., Attisano, L., Rossant, J. and Wrana, J. L. (2001). FoxH1 (Fast) functions to specify the anterior primitive streak in the mouse. *Genes Dev.* **15**, 1257-1271.

Hou, J., Charters, A. M., Lee, S. C., Zhao, Y., Wu, M. K., Jones, S. J. M., Marra, M. A. and Hoodless, P. A. (2007). A systematic screen for genes expressed in definitive endoderm by Serial Analysis of Gene Expression (SAGE). *BMC Dev. Biol.* **7**, 92.

Kanai, Y., Kanai-Azuma, M., Noce, T., Saido, T. C., Shiroishi, T., Hayashi, Y. and Yazaki, K. (1996). Identification of two Sox17 messenger RNA isoforms, with and without the high mobility group box region, and their differential expression in mouse spermatogenesis. *J. Cell Biol.* **133**, 667-681.

Kanai-Azuma, M., Kanai, Y., Gad, J. M., Tajima, Y., Taya, C., Kurohmaru, M., Sanai, Y., Yonekawa, H., Yazaki, K., Tam, P. P. et al. (2002). Depletion of definitive gut endoderm in Sox17-null mutant mice. *Development* **129**, 2367-2379.

Kimura, W., Yasugi, S. and Fukuda, K. (2007). Regional specification of the endoderm in the early chick embryo. *Dev. Growth Differ.* **49**, 365-372.

Kraus, M. R. C. and Grapin-Botton, A. (2012). Patterning and shaping the endoderm in vivo and in culture. *Curr. Opin. Genet. Dev.* **22**, 347-353.

Lawson, K. A. (1999). Fate mapping the mouse embryo. *Int. J. Dev. Biol.* **43**, 773-775.

Lewis, S. L. and Tam, P. P. L. (2006). Definitive endoderm of the mouse embryo: formation, cell fates, and morphogenetic function. *Dev. Dyn.* **235**, 2315-2329.

Li, Y., Rankin, S. A., Sinner, D., Kenny, A. P., Krieg, P. A. and Zorn, A. M. (2008). Sfrp5 coordinates foregut specification and morphogenesis by antagonizing both canonical and noncanonical Wnt11 signaling. *Genes Dev.* **22**, 3050-3063.

Martín, M., Gallego-Llamas, J., Ribes, V., Kedinger, M., Niederreither, K., Chambon, P., Dollé, P. and Gradwohl, G. (2005). Dorsal pancreas agenesis in retinoic acid-deficient Raldh2 mutant mice. *Dev. Biol.* **284**, 399-411.

McKnight, K. D., Hou, J. and Hoodless, P. A. (2010). Foxh1 and Foxa2 are not required for formation of the midgut and hindgut definitive endoderm. *Dev. Biol.* **337**, 471-481.

McLin, V. A., Rankin, S. A. and Zorn, A. M. (2007). Repression of Wnt/beta-catenin signaling in the anterior endoderm is essential for liver and pancreas development. *Development* **134**, 2207-2217.

Mic, F. A., Haselbeck, R. J., Cuenca, A. E. and Duester, G. (2002). Novel retinoic acid generating activities in the neural tube and heart identified by conditional rescue of Raldh2 null mutant mice. *Development* **129**, 2271-2282.

Mochida, Y., Parisuthiman, D., Kaku, M., Hanai, J.-I., Sukhatme, V. P. and Yamauchi, M. (2006). Nephrocan, a novel member of the small leucine-rich repeat protein family, is an inhibitor of transforming growth factor-beta signaling. *J. Biol. Chem.* **281**, 36044-36051.

Molotkov, A., Molotkova, N. and Duester, G. (2005). Retinoic acid generated by Raldh2 in mesoderm is required for mouse dorsal endodermal pancreas development. *Dev. Dyn.* **232**, 950-957.

Norris, D. P., Brennan, J., Bikoff, E. K. and Robertson, E. J. (2002). The Foxh1-dependent autoregulatory enhancer controls the level of Nodal signals in the mouse embryo. *Development* **129**, 3455-3468.

Nowotschin, S. and Hadjantonakis, A.-K. (2010). Cellular dynamics in the early mouse embryo: from axis formation to gastrulation. *Curr. Opin. Genet. Dev.* **20**, 420-427.

Ovcharenko, I., Loots, G. G., Nobrega, M. A., Hardison, R. C., Miller, W. and Stubbs, L. (2005). Evolution and functional classification of vertebrate gene deserts. *Genome Res.* **15**, 137-145.

Rossant, J., Zirngibl, R., Cado, D., Shago, M. and Giguere, V. (1991). Expression of a retinoic acid response element-hsplacZ transgene defines specific domains of transcriptional activity during mouse embryogenesis. *Genes Dev.* **5**, 1333-1344.

Saijoh, Y., Adachi, H., Sakuma, R., Yeo, C.-Y., Yashiro, K., Watanabe, M., Hashiguchi, H., Mochida, K., Ohishi, S., Kawabata, M. et al. (2000). Left-right asymmetric expression of lefty2 and nodal is induced by a signaling pathway that includes the transcription factor FAST2. *Mol. Cell* **5**, 35-47.

Sakai, Y., Meno, C., Fujii, H., Nishino, J., Shiratori, H., Saijoh, Y., Rossant, J. and Hamada, H. (2001). The retinoic acid-inactivating enzyme CYP26 is essential for establishing an uneven distribution of retinoic acid along the anterio-posterior axis within the mouse embryo. *Genes Dev.* **15**, 213-225.

Saund, R. S., Kanai-Azuma, M., Kanai, Y., Kim, I., Lucero, M. T. and Saijoh, Y. (2012). Gut endoderm is involved in the transfer of left-right asymmetry from the node to the lateral plate mesoderm in the mouse embryo. *Development* **139**, 2426-2435.

Sherwood, R. I., Maehr, R., Mazzoni, E. O. and Melton, D. A. (2011). Wnt signaling specifies and patterns intestinal endoderm. *Mech. Dev.* **128**, 387-400.

Sirbu, I. O. and Duester, G. (2006). Retinoic-acid signalling in node ectoderm and posterior neural plate directs left-right patterning of somitic mesoderm. *Nat. Cell Biol.* **8**, 271-277.

Sirbu, I. O., Gresh, L., Barra, J. and Duester, G. (2005). Shifting boundaries of retinoic acid activity control hindbrain segmental gene expression. *Development* **132**, 2611-2622.

Stafford, D. and Prince, V. E. (2002). Retinoic acid signaling is required for a critical early step in zebrafish pancreatic development. *Curr. Biol.* **12**, 1215-1220.

Teo, A. K. K., Arnold, S. J., Trotter, M. W. B., Brown, S., Ang, L. T., Chng, Z., Robertson, E. J., Dunn, N. R. and Vallier, L. (2011). Pluripotency factors regulate definitive endoderm specification through eomesodermin. *Genes Dev.* **25**, 238-250.

Tiso, N., Filippi, A., Pauls, S., Bortolussi, M. and Argenton, F. (2002). BMP signalling regulates anteroposterior endoderm patterning in zebrafish. *Mech. Dev.* **118**, 29-37.

Turkson, J., Kim, J. S., Zhang, S., Yuan, J., Huang, M., Glenn, M., Haura, E., Sebti, S., Hamilton, A. D. and Jove, R. (2004). Novel peptidomimetic inhibitors of signal transducer and activator of transcription 3 dimerization and biological activity. *Mol. Cancer Ther.* **3**, 261-269.

Uehara, M., Yashiro, K., Takaoka, K., Yamamoto, M. and Hamada, H. (2009). Removal of maternal retinoic acid by embryonic CYP26 is required for correct Nodal expression during early embryonic patterning. *Genes Dev.* **23**, 1689-1698.

Underhill, T. M., Cash, D. E. and Linney, E. (1994). Constitutively active retinoid receptors exhibit interfamily and intrafamily promoter specificity. *Mol. Endocrinol.* **8**, 274-285.

Vincent, S. D., Dunn, N. R., Hayashi, S., Norris, D. P. and Robertson, E. J. (2003). Cell fate decisions within the mouse organizer are governed by graded Nodal signals. *Genes Dev.* **17**, 1646-1662.

Wells, J. M. and Melton, D. A. (2000). Early mouse endoderm is patterned by soluble factors from adjacent germ layers. *Development* **127**, 1563-1572.

Wendling, O., Dennefeld, C., Chambon, P. and Mark, M. (2000). Retinoid signaling is essential for patterning the endoderm of the third and fourth pharyngeal arches. *Development* **127**, 1553-1562.

Wills, A., Dickinson, K., Khokha, M. and Baker, J. C. (2008). Bmp signaling is necessary and sufficient for ventrolateral endoderm specification in Xenopus. *Dev. Dyn.* **237**, 2177-2186.

Xiang, P., Lo, C., Argiropoulos, B., Lai, C. B., Rouhi, A., Imren, S., Jiang, X., Mager, D. and Humphries, R. K. (2010). Identification of E74-like factor 1 (ELF1) as a transcriptional regulator of the Hox cofactor MEIS1. *Exp. Hematol.* **38**, 798-808.e2.

Yamamoto, M., Meno, C., Sakai, Y., Shiratori, H., Mochida, K., Ikawa, Y., Saijoh, Y. and Hamada, H. (2001). The transcription factor FoxH1 (FAST) mediates Nodal signaling during anterior-posterior patterning and node formation in the mouse. *Genes Dev.* **15**, 1242-1256.

Yamamoto, M., Mine, N., Mochida, K., Sakai, Y., Saijoh, Y., Meno, C. and Hamada, H. (2003). Nodal signaling induces the midline barrier by activating Nodal expression in the lateral plate. *Development* **130**, 1795-1804.

Yamanaka, Y., Lanner, F. and Rossant, J. (2010). FGF signal-dependent segregation of primitive endoderm and epiblast in the mouse blastocyst. *Development* **137**, 715-724.

Zorn, A. M. and Wells, J. M. (2009). Vertebrate endoderm development and organ formation. *Annu. Rev. Cell Dev. Biol.* **25**, 221-251.